Proceedings of the 2009 IEEE International Conference on Systems, Man, and Cybernetics
San Antonio, TX, USA - October 2009

DYNAMIC MODELING AND CONTROL OF THE OMEGA-3 PARALLEL MANIPULATOR

Collins F. Adetu, Carl A. Moore, Jr.*, Rodney G. Roberts
Dept. of Electrical and Computer Engineering, *Dept. of Mechanical Engineering
Florida A&M – Florida State University
Tallahassee, FL 32310-6046, USA
e-mail: {adetuco, camoore, rroberts}@eng.fsu.edu

Abstract*— Parallel manipulators are widely used in industrial applications due to their rigid structures and ability to perform automated tasks at high speeds. However, because the links on a parallel manipulator are mechanically coupled, solving its kinematics and dynamics equations can be more difficult than for its serial counterpart. Nevertheless, the inverse kinematics and inverse dynamics models are a critical component of a manipulator's controller. Specifically, a more computationally simple formulation of the inverse kinematics and dynamics is necessary to achieve efficient and fast manipulator control. In this paper, both the inverse kinematics and dynamics equations for the Omega-3, a three degree-of-freedom (3-DOF) parallel manipulator, are developed. For the inverse kinematics problem, the concept of loop closure equations is used to simplify the analysis. The virtual work principle is used to create a numerically simple inverse dynamics model. Using the inverse kinematics and dynamics model, a trajectory tracking controller is implemented on the manipulator and the resulting experiments reveal good tracking behavior. *(Abstract)

Keywords*—parallel manipulators, dynamic modeling, dynamic control, trajectory tracking. *(key words)

I. INTRODUCTION

Over recent years the interest in parallel manipulators has been on the rise. These manipulators play a vital role not only in industrial automation but other applications as well. For example, there have been studies that suggest the use of parallel manipulators for cardiopulmonary resuscitation (CPR) [1], flight simulators, shakers – used in the study of earthquakes [2], and even image-guided orthopedic surgery [3]. These are just a few applications of parallel manipulators, [4] and [5] provides an extensive list of other parallel manipulators and their applications. The versatility of the parallel manipulator, as highlighted by some of its applications mentioned previously, is innately due to its architecture. Parallel manipulators have more than one link directly coupled to the end-effector creating a closed-loop. This closed-loop architecture, allows for a more rigid structure, therefore, making the parallel manipulator quicker, more accurate, more energy efficient [6], and having a higher load carrying-capacity when compared to its serial counterparts.

Although parallel manipulators possess a high dexterity, the presence of its closed-loop structure and redundant joints make it difficult to develop an inverse dynamic model, which is essential in creating a model-based control scheme for the manipulator. Several approaches have been proposed in developing an inverse dynamic model for parallel manipulators, amongst them is the Newton-Euler's method [7, 8, 9] and the Lagrangian formulation [10, 11, 12, 13]. Unfortunately, the numerous constraints and nonlinear relationship between the actuated joints and end-effector, renders both the Newton-Euler and Lagrangian method computationally laborious. In order to perform dynamic analysis with less complexity, a technique known as the principle of virtual work is employed [14]. This method has been applied to the development of inverse dynamic models of the Stewart-Gough manipulator [16], the DELTA manipulator [15], and other special parallel manipulators [17, 18].

In this paper, a computationally simple inverse dynamic model is developed for the Omega-3 parallel robot – a progeny of the DELTA parallel robot [19]. The model is developed using the principle of virtual work, taking advantage of the fact that this technique does not require the explicit knowledge of constraint equations in order to obtain the manipulator's dynamics. To reduce the complexity of the dynamic analysis, a simplifying hypothesis [15] is employed. The opening section of the paper provides an adequate description of the Omega-3 robot. In subsequent sections, the inverse kinematics, Jacobian, and acceleration analysis are discussed. The latter sections focus on the simplifying hypothesis and derivation of the inverse dynamic model. Eventually, using the model developed a proportional-derivative (PD) trajectory tracking controller is incorporated and trajectory tracking results are revealed.

II. DESCRIPTION OF THE OMEGA-3 PARALLEL ROBOT

Fig. 1 shows a diagram of the Omega-3 parallel manipulator used in this research. The manipulator's structure is based on that of the DELTA manipulator developed by Clavel [19]. The Omega-3 has three identical kinematic chains, all linked at the triangular traveling plate. Each kinematic chain consists of a semi-circular arm and a pair of parallel light-weight rods that connects the semi-circular arms to the triangular traveling plate and payload. The motors of the manipulator are housed at the base and actuate the semi-circular arms. Just like its predecessor (the DELTA manipulator), the kinematic chains of the Omega-3 are of type RRPaR, where R and Pa represent revolute joint and parallelogram respectively.

978-1-4244-2794-9/09/$25.00 ©2009 IEEE

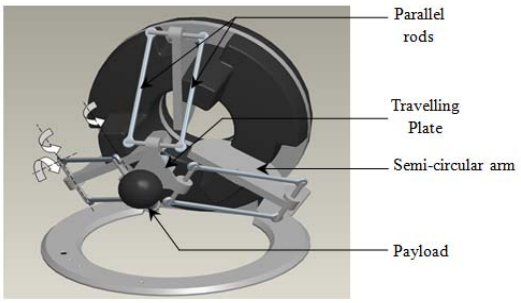

Figure 1. The Omega_3 Parallel manipulator.

Only the revolute joints at the base of the device are actuated, all other joints are considered passive. Fig. 1 shows the axis of rotation for the actuated semi-circular arm and the two orthogonal axis of rotation for the passive parallel rod joints. The resulting motion of the manipulator is purely translational, due to the presence of its parallel rods.

III. MANIPULATOR KINEMATICS

Before we begin the inverse kinematics analysis, certain geometric parameters have to be defined. Fig. 2 provides an appropriate description of all parameters referred to in this section of the paper, while Table I describes the values of each parameter.

TABLE I. KINEMATIC PARAMETERS FOR THE OMEGA-3 MANIPULATOR

Parameter	*Length (mm)*
L_A	70.00
L_B	146.00
R_A	75.00
R_B	35.25

L_A and L_B are the radius of the semi-circular arm and the length of the parallel link respectively. The absolute reference frame *{O}* is located at the center of the circular base of the manipulator, with each i^{th} chain fixed at an angle $\emptyset_i = 2\pi(i-1)/3$ where i= 1, 2, and 3. The actuated angle located at joint A_i is defined as θ_i and is measured as illustrated in fig. 2(b). Although there have been inverse kinematic models expressed using passive joint angles [20, 21], the kinematic analysis discussed here would only involve actuated joint angles, θ_i. By leaving out the passive joint angles, a less complicated formulation of the inverse kinematics model can be developed with fewer unknowns to solve. To solve for the inverse kinematics, the following loop-closure equation is considered:

$$\overrightarrow{B_\iota C_\iota} = \overrightarrow{A_\iota C_\iota} - \overrightarrow{A_\iota B_\iota}. \quad (1)$$

This loop-closure equation is intentionally selected as a basis for solving the inverse kinematics of the parallel manipulator in question because of its compact form. The more general form of the loop-closure equation is shown below:

$$\overrightarrow{OP} + \overrightarrow{PC_\iota} = \overrightarrow{OA_\iota} + \overrightarrow{A_\iota B_\iota} + \overrightarrow{B_\iota C_\iota}. \quad (2)$$

Note that (1) is a simplified version of (2) and can be derived by simple vector algebraic manipulation of (2). Because the traveling plate is always parallel to the base of the manipulator, each kinematic chain can be translated by a distance R=R_A-R_B as shown in fig. 2(b). Therefore, allowing frame $\{C_i\}$ to coincide with the end-effector frame *{P}*, $\{B_i\}$ becomes $\{B'_i\}$, and $\{A_i\}$ becomes $\{A'_i\}$.

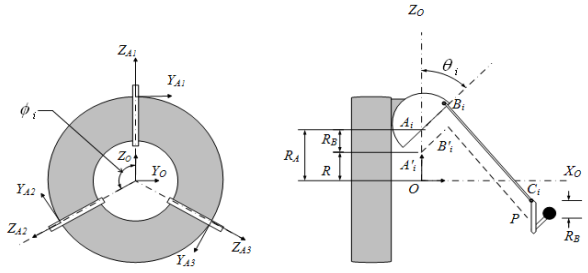

(a) Front view (b) Side view

Figure 2. Front and side view of the Omega-3 manipulator.

This translation simplifies the analysis a great deal without affecting the results as shown in [15]. With this in mind, (1) can now be written as:

$$\overrightarrow{B'_\iota P} = \overrightarrow{A'_\iota P} - \overrightarrow{A'_\iota B'_\iota}. \quad (3)$$

Taking the magnitude of (3) and squaring both sides we obtain,

$$\|B'_i P\|^2 = \|A'_i P\|^2 + \|A'_i B'_i\|^2 - 2\,\overrightarrow{A'_\iota P}.\overrightarrow{A'_\iota B'_\iota}, \quad (4)$$

where,

$$\|B'_i P\| = L_B, \quad (5)$$

$$\|A'_i B'_i\| = L_A, \quad (6)$$

$$\overrightarrow{A'_\iota B'_\iota} = {}^{O}_{A'_i}R\,[L_A \sin\theta_i \quad 0 \quad L_A \cos\theta_i]^T, \quad (7)$$

$$\overrightarrow{A'_\iota P} = \overrightarrow{OP} - {}^{O}_{A'_i}R\overrightarrow{OA'_\iota}, \quad (8)$$

where,

$${}^{O}_{A'_i}R = \begin{bmatrix} 1 & 0 & 0 \\ 0 & \cos\emptyset_i & -\sin\emptyset_i \\ 0 & \sin\emptyset_i & \cos\emptyset_i \end{bmatrix}, \quad (9)$$

$$\overrightarrow{OA'_\iota} = [0 \quad 0 \quad R]^T, \quad (10)$$

$$\overrightarrow{OP} = [P_x \quad P_y \quad P_z]^T. \quad (11)$$

The rotational matrix, ${}^{O}_{A'_i}R$, specifies the orientation of frame $\{A'_i\}$ relative to the absolute reference frame *{O}*, note both $\overrightarrow{A'_\iota B'_\iota}$ and $\overrightarrow{A'_\iota P}$ are described relative to frame *{O}*. P_x, P_y, and P_z are the end-effector position, and R=R_A-R_B as defined previously.

With the parameters defined above and the end-effector position, P_x, P_y, and P_z known, all three kinematic chains can be solved from (4) to obtain the actuated angles: θ_1, θ_2, and θ_3.

A. Velocity

The Jacobian, J, provides a linear mapping between end-effector velocities and joint velocities. Equation (12) illustrates this relationship:

$$\dot{\boldsymbol{X}} = J\dot{\boldsymbol{\Theta}}, \tag{12}$$

where, $\dot{\boldsymbol{\Theta}}$ is an m-dimensional vector of joint rates, $\dot{\boldsymbol{X}}$ is an n-dimensional vector of the end-effector velocity, and J is an $n \times m$ Jacobian matrix. In the case of the Omega-3 manipulator, the Jacobian matrix is a 3×3 square matrix. To begin the velocity analysis, the equation below is chosen for each ith chain:

$$\|B'_i P\|^2 - {L_B}^2 = 0. \tag{13}$$

This equation can be interpreted physically as meaning the length of the manipulator's parallel rods are the same for all three kinematic chains. Replacing $\overrightarrow{B'_i P}$ with $\boldsymbol{u_i}$, we can rewrite (13) as:

$$\boldsymbol{u_i}^{\boldsymbol{T}} \cdot \boldsymbol{u_i} - {L_B}^2 = 0, \tag{14}$$

$\boldsymbol{u_i}$ can be rewritten as:

$$\boldsymbol{u_i} = \overrightarrow{OP} - {}^{O}_{A'_i}R(\overrightarrow{OA'_i} + \overrightarrow{A'_i B'_i}). \tag{15}$$

After making necessary substitutions as defined by (7), (10), and (11) we get:

$$\boldsymbol{u_i} = \begin{bmatrix} P_x \\ P_y \\ P_z \end{bmatrix} - {}^{O}_{A'_i}R\left(\begin{bmatrix} 0 \\ 0 \\ R \end{bmatrix} + \begin{bmatrix} L_A \sin\theta_i \\ 0 \\ L_A \cos\theta_i \end{bmatrix}\right). \tag{16}$$

Taking the time derivative of (14), leads to:

$$\boldsymbol{u_i}^{\boldsymbol{T}} \cdot \dot{\boldsymbol{u}}_{\boldsymbol{i}} - \dot{\boldsymbol{u}}_{\boldsymbol{i}}^{\boldsymbol{T}} \cdot \boldsymbol{u_i} = 0. \tag{17}$$

Due to the dot product's commutative property (17) can be rewritten as,

$$\boldsymbol{u_i}^{\boldsymbol{T}} \cdot \dot{\boldsymbol{u}}_{\boldsymbol{i}} = 0, \tag{18}$$

$\dot{\boldsymbol{u}}_{\boldsymbol{i}}$ is given by,

$$\dot{\boldsymbol{u}}_{\boldsymbol{i}} = \begin{bmatrix} V_x \\ V_y \\ V_z \end{bmatrix} + {}^{O}_{A'_i}R\left(\begin{bmatrix} -L_A \cos\theta_i \\ 0 \\ L_A \sin\theta_i \end{bmatrix}\right)\dot{\boldsymbol{\Theta}} = \dot{\boldsymbol{X}} + b_i\dot{\boldsymbol{\Theta}}. \tag{19}$$

Equation (19) is multiplied by $\boldsymbol{u_i}^{\boldsymbol{T}}$ to give a similar result as (18),

$$\boldsymbol{u_i}^{\boldsymbol{T}} \cdot \dot{\boldsymbol{u}}_{\boldsymbol{i}} = \boldsymbol{u_i}^{\boldsymbol{T}}\dot{X} + \boldsymbol{u_i}^{\boldsymbol{T}} b_i \dot{\boldsymbol{\Theta}} = 0, \tag{20}$$

where,

$$b_i = {}^{O}_{A'_i}R\left(\begin{bmatrix} -L_A \cos\theta_i \\ 0 \\ L_A \sin\theta_i \end{bmatrix}\right). \tag{21}$$

Equation (20) can be written in vector form, with the values for i as 1, 2, and 3, substituted to obtain the following expression,

$$\begin{bmatrix} {u_1}^T \\ {u_2}^T \\ {u_3}^T \end{bmatrix}\dot{\boldsymbol{X}} + \begin{bmatrix} {u_1}^T b_1 & 0 & 0 \\ 0 & {u_2}^T b_2 & 0 \\ 0 & 0 & {u_3}^T b_3 \end{bmatrix}\dot{\boldsymbol{\Theta}} = \begin{bmatrix} 0 \\ 0 \\ 0 \end{bmatrix}, \tag{22}$$

where, $\dot{\boldsymbol{\Theta}}$ is the actuated joint velocities, $[\dot{\theta}_1 \quad \dot{\theta}_2 \quad \dot{\theta}_3]^T$, and $\dot{\boldsymbol{X}}$ is the end-effector velocity, $[V_x \quad V_y \quad V_z]^T$. Rearranging (22) to look like (12), the Jacobian becomes:

$$J = -\begin{bmatrix} {u_1}^T \\ {u_2}^T \\ {u_3}^T \end{bmatrix}^{-1}\begin{bmatrix} {u_1}^T b_1 & 0 & 0 \\ 0 & {u_2}^T b_2 & 0 \\ 0 & 0 & {u_3}^T b_3 \end{bmatrix}. \tag{23}$$

From the expression obtained for the Jacobian, a major difference between serial and parallel manipulators is observed. Unlike the Jacobian of serial manipulators which is dependent only on joint positions, the Jacobian of parallel manipulators depends on both joint positions and the end-effector position.

B. Acceleration

Next, an expression for the derivative of the Jacobian matrix, $\dot{J}$, is obtained. In order to calculate the derivative of the Jacobian matrix, the relationship between the manipulator's joint accelerations and end-effector acceleration is examined. This relationship is expressed in its general form in (24) by differentiating (12),

$$\ddot{\boldsymbol{X}} = \dot{J}\dot{\boldsymbol{\Theta}} + J\ddot{\boldsymbol{\Theta}}. \tag{24}$$

Equation (22) is an explicit form of (12), therefore, the derivative of (22) can be taken to obtain an explicit form of (24). Differentiating (22) and rearranging the equation results in the following:

$$\begin{bmatrix} {u_1}^T \\ {u_2}^T \\ {u_3}^T \end{bmatrix}\ddot{\boldsymbol{X}} = -\begin{bmatrix} \dot{u}_1^T \\ \dot{u}_2^T \\ \dot{u}_3^T \end{bmatrix}\dot{\boldsymbol{X}} - K\dot{\boldsymbol{\Theta}} - L\ddot{\boldsymbol{\Theta}}, \tag{25}$$

where,

$$K = \begin{bmatrix} {u_1}^T\dot{b}_1 + \dot{u}_1^T b_1 & 0 & 0 \\ 0 & {u_2}^T\dot{b}_2 + \dot{u}_2^T b_2 & 0 \\ 0 & 0 & {u_3}^T\dot{b}_3 + \dot{u}_3^T b_3 \end{bmatrix},$$

$$L = \begin{bmatrix} {u_1}^T b_1 & 0 & 0 \\ 0 & {u_2}^T b_2 & 0 \\ 0 & 0 & {u_3}^T b_3 \end{bmatrix}.$$

Substituting (12) for $\dot{\boldsymbol{X}}$ and (23) for the coefficient of $\ddot{\boldsymbol{\Theta}}$, we get,

$$\ddot{\boldsymbol{X}} = -\begin{bmatrix} {u_1}^T \\ {u_2}^T \\ {u_3}^T \end{bmatrix}^{-1}\left(\begin{bmatrix} \dot{u}_1^T \\ \dot{u}_2^T \\ \dot{u}_3^T \end{bmatrix}J + K\right)\dot{\boldsymbol{\Theta}} + J\ddot{\boldsymbol{\Theta}}. \tag{26}$$

Comparing (26) with (24) we see both equations are similar and it is obvious that, $\dot{J}$, is the term being multiplied by $\dot{\boldsymbol{\Theta}}$. Hence,

$$\dot{J} = -\begin{bmatrix} {u_1}^T \\ {u_2}^T \\ {u_3}^T \end{bmatrix}^{-1}\left(\begin{bmatrix} \dot{u}_1^T \\ \dot{u}_2^T \\ \dot{u}_3^T \end{bmatrix}J + K\right) \tag{27}$$

IV. Manipulator Dynamics

For a manipulator with n actuated joints, its rigid body dynamics, assuming no user force applied on the end-effector, is governed by the following equation:

$$\tau = M(\boldsymbol{\Theta})\ddot{\boldsymbol{\Theta}} + V\left(\boldsymbol{\Theta}, \dot{\boldsymbol{\Theta}}\right) + G(\boldsymbol{\Theta}) \tag{28}$$

where $M(\boldsymbol{\Theta})$ is the $n \times n$ mass matrix of the manipulator and a function of the joint angles $\boldsymbol{\Theta}$, $V\left(\boldsymbol{\Theta}, \dot{\boldsymbol{\Theta}}\right)$ is an $n \times 1$ vector of centrifugal and Coriolis terms and a function of both joint angles $\boldsymbol{\Theta}$ and joint velocities $\dot{\boldsymbol{\Theta}}$, $G(\boldsymbol{\Theta})$ is an $n \times 1$ vector of gravity terms and a function of joint position $\boldsymbol{\Theta}$, and τ is an $n \times 1$ vector of joint torques. Table II provides the masses of the different members of the Omega-3 manipulator.

TABLE II. Masses associated with the OMEGA-3 Manipulator

Parameter	*Mass (g)*
$m_{PAYLOAD}$	70.00
m_P	110.00
m_R	34.93
m_{SC}	100.00

A. The Principle of Virtual Work

In order to obtain (28) we employ the principle of virtual work. The principle states that at equilibrium, the virtual work, δW, done by all external forces, F, acting on a body during any virtual displacement, δr, consistent with the structural constraints imposed on the body is equal to zero. This principle is illustrated mathematically below:

$$\delta W = \sum_{i=1}^{N} F_i \cdot \delta r_i = 0 \tag{29}$$

In (29), only external forces are considered, all internal forces, i.e. constraint and reaction forces are ignored because no virtual work is done by these forces. The virtual work principle is traditionally used to solve static problems. However, for a system that is not at rest, the force (*inertia force*) as a result of the body's mass, m, accelerating at rate, a, is included in (29). This extension of the principle of virtual work for dynamic cases is known as D'Alembert's principle [22]. Equation (30) is an extension of (29) with the inertia force included:

$$\delta W = \sum_{i=1}^{N} (F_i - m_i a_i) \cdot \delta r_i = 0. \tag{30}$$

For a rigid body that is capable of both translational and rotational motion (30) is generally written as:

$$\delta W = \sum_{i=1}^{N} [(F_i - m_i a_i) \cdot \delta r_i + (\tau_i - I\ddot{\theta})\delta\theta] = 0, \tag{31}$$

where, τ is the external torque acting on the body, I is the moment of inertia, $\ddot{\theta}$ the angular acceleration, and $\delta\theta$ is the virtual angular displacement.

B. Simplifying Hypothesis

The Omega-3 parallel manipulator, just like its DELTA predecessor, consists of parallel rods. These parallel members add to the complexity of the dynamic model. However, because these rods are built from lightweight aluminum alloy, it is possible to simplify the dynamic problem by applying propositions discussed in [15] which neglects the rotational inertia of the parallel rods and divides their masses into two portions concentrated at the two joint extremities. Therefore, half of the rod's mass is centered at the upper extremity (i.e. the joint where the semi-circular member meets the parallel rods), while the other half is centered at the lower extremity (i.e. the joint where the parallel rods meet the moving triangular platform). With this simplifying hypothesis applied to the system, the manipulator is reduced to only two members – the three semi-circular arms and the end-effector plate.

C. Dynamics Analysis

1) The End-Effector: The end-effector portion consists of the travelling plate, the payload, and the concentrated masses of the parallel links. The mass of this portion, m_E, is expressed as follows:

$$m_E = m_{PAYLOAD} + m_P + 3(1/2m_R) \tag{32}$$

where, $m_{PAYLOAD}$ is the mass of the payload, m_P is the mass of the travelling plate, and m_R is the mass of a pair of parallel rods. Due to the architecture of the Omega-3 manipulator, the orientation of end-effector frame is always parallel to the reference frame *{O}*. Therefore, we can neglect rotational motion terms for the end-effector in (31). The only forces acting on the end-effector are the force due to gravity, F_G, and the inertia force, F_A, due to the acceleration of the end-effector. The principle of virtual work equation for the end-effector can then be written in its vector form as:

$$(\boldsymbol{F}_G - m_E \boldsymbol{a}_E) \cdot \delta \boldsymbol{r}_E = 0, \tag{33}$$

where, $\boldsymbol{F}_G = m_E[0 \quad 0 \quad -\mathrm{g}]^T$, g is the acceleration due to gravity, $\boldsymbol{a}_E$ is the acceleration vector of the end-effector, and $\delta \boldsymbol{r}_E$ is the virtual displacement of the end-effector.

2) Semi-Circular Arms: This member consists of the semi-circular sector and the concentrated point masses of the parallel rods. Three torques act on the semi-circular arms at any point in time: the torque τ_{CM} due to gravity acting on the center of mass, the torque τ_A due to the actuator, and the torque due to the moment of inertia I about the axis of rotation. The virtual work equation of the semi-circular arm is then expressed as follows:

$$(\tau_A + \tau_{CM} - I\ddot{\theta})\delta\theta = 0. \tag{34}$$

To obtain the torque due to gravity, the center of mass of the composite semi-circular arm, which includes the concentrated point masses of the parallel rods, first has to be calculated. Let $\vec{R}_{CM}$ represent the location of the center of mass of the composite member:

$$\vec{R}_{CM} = \frac{m_{SC}\vec{r}_{SC} + 1/2m_R\vec{r}_R}{m_{SC} + 1/2m_R}, \tag{35}$$

where, m_{SC} is the mass of the semi-circular sector (*without the concentrated parallel rod mass*), $1/2m_R$ is the concentrated point mass of the parallel rods, $\vec{r}_{SC}$ and $\vec{r}_R$ is the location of their center of mass respectively relative to the center of rotation. Taking into consideration the fact that the semi-circular arm rotates about its y-axis by θ_i as shown in fig. 2(b), the vector $\vec{R}_{CM}$ is rotated accordingly. Also due to the difference in orientation of the individual semi-circular arms from the reference frame *{O}* by $\emptyset_i$ as shown in fig. 2(a), the

gravity acting on each semi-circular arm is expressed by multiplying the gravity vector defined in the reference frame by the transpose of the rotation matrix defined in (9). Therefore, the torque due to gravity on the semi-circular arm is calculated as shown:

$$\tau_{\mathrm{CM}} = R_y(\theta_i)\vec{R}_{CM} \times (m_{SC} + 1/2m_R)[{}^{O}_{A'_i}R]^T\vec{g}. \quad (36)$$

The moment of inertia of the composite semi-circular arm can be calculated by adding the moment of inertia of the semi-circle (without the point mass of the parallel rods) to the moment of inertia of the point mass. Considering the axis of rotation is not coincident with the center of mass of the semi-circle, the parallel axis theorem is used to calculate the inertia of the semi-circle, I_{SC}:

$$I_{SC} = I_o + m_{SC}d^2, \quad (37)$$

where, I_o is the moment of inertia at the center of mass of the semi-circle, m_{SC} is the mass of the semi-circle (excluding the point mass of the rods), and d is the distance from the point of rotation to the center of mass. Adding the moment of inertia, I_{PR}, of the concentrated point mass of the parallel rods, the inertia of the composite semi-circular arm is defined as:

$$I = I_{SC} + I_{PR}. \quad (38)$$

D. Complete Manipulator Dynamics

With the dynamic parameters for the individual components of the manipulator calculated, the complete manipulator dynamics can now be developed. Recall from (31), the sum of all virtual work done on the system by all external forces and torques must be equal to zero. Therefore, adding (33) to (34) we have,

$$(\boldsymbol{F}_G - m_E\boldsymbol{a}_E) \cdot \delta\boldsymbol{r}_E + \left(\boldsymbol{\Gamma}_{\mathrm{A}} + \boldsymbol{\Gamma}_{\mathrm{CM}} - I\ddot{\boldsymbol{\Theta}}\right)\delta\boldsymbol{\Theta} = \mathbf{0}, \quad (39)$$

where, $\boldsymbol{\Gamma}_{\mathrm{A}}$ is a vector of actuator torques, $[\tau_{A1} \quad \tau_{A2} \quad \tau_{A3}]^T$, for all three joints, $\boldsymbol{\Gamma}_{\mathrm{CM}}$ is a vector of torques due to the gravity, $[\tau_{CM1} \quad \tau_{CM2} \quad \tau_{CM3}]^T$, for all three semi-circular arms, and $\ddot{\boldsymbol{\Theta}}$ is a vector of angular accelerations, $[\ddot{\theta}_1 \quad \ddot{\theta}_2 \quad \ddot{\theta}_3]^T$. Taking the dot product of the translation force terms, $(\boldsymbol{F}_G - m_E\boldsymbol{a}_E)$, and translational displacement, $\delta\boldsymbol{r}_E$, (39) is rewritten as shown:

$$(\boldsymbol{F}_G{}^T - m_E\boldsymbol{a}_E{}^T)\delta\boldsymbol{r}_E + \left(\boldsymbol{\Gamma}_{\mathrm{A}} + \boldsymbol{\Gamma}_{\mathrm{CM}} - I\ddot{\boldsymbol{\Theta}}\right)\delta\boldsymbol{\Theta} = \mathbf{0}. \quad (40)$$

By substituting (12) and (24) for $\delta\boldsymbol{r}_E$ and $\boldsymbol{a}_E$ respectively, (40) becomes,

$$\left(\boldsymbol{F}_G{}^T - m_E\left(\dot{J}\dot{\boldsymbol{\Theta}} + J\ddot{\boldsymbol{\Theta}}\right)^T\right)J\delta\boldsymbol{\Theta} + \left(\boldsymbol{\Gamma}_{\mathrm{A}} + \boldsymbol{\Gamma}_{\mathrm{CM}} - I\ddot{\boldsymbol{\Theta}}\right)\delta\boldsymbol{\Theta} = \mathbf{0}. \quad (41)$$

Further simplification and rearrangement of (41) yields,

$$\boldsymbol{\Gamma}_{\mathrm{A}} = (I + J^T m_E J)\ddot{\boldsymbol{\Theta}} + J^T m_E\dot{J}\dot{\boldsymbol{\Theta}} - \boldsymbol{\Gamma}_{\mathrm{CM}} - J^T\boldsymbol{F}_G, \quad (42)$$

comparing (42) with (28), the following dynamic parameters can be extracted,

$$M(\boldsymbol{\Theta}) = I + J^T m_E J,$$
$$V(\boldsymbol{\Theta}, \dot{\boldsymbol{\Theta}}) = J^T m_E\dot{J}\dot{\boldsymbol{\Theta}},$$
$$G(\boldsymbol{\Theta}) = -(\boldsymbol{\Gamma}_{\mathrm{CM}} + J^T\boldsymbol{F}_G).$$

V. Trajectory Tracking Results

A trajectory tracking controller is implemented using a Proportional-Derivative (PD) feedback scheme and the manipulator's dynamics, as illustrated in fig. 3. The desired task-space trajectory is described by (43) and its parametric plot in the y-z plane is shown in fig. 4(a).

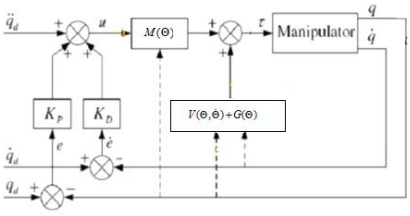

Figure 3. PD feedback controller scheme.

$$x(t) = 0.1,$$
$$y(t) = 0.06\cos(\pi t), \quad (43)$$
$$z(t) = 0.06\sin(2\pi t).$$

The desired task-space trajectory is converted to joint-space, and its position and velocity in joint space are shown in fig. 4(b) and (c) respectively.

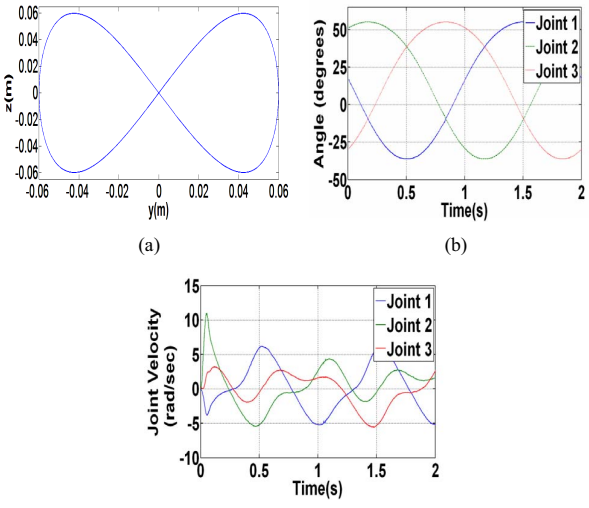

Figure 4. (a) Parametric plot of desired task-space trajectory, (b) desired joint positions, and (c) desired joint velocities

Fig. 5(a) shows a parametric plot of the desired and actual task-space trajectory path in the y-z plane and fig. 5(b) shows the task-space position error plot. The actuated joint torques are also shown in fig. 5(c). It is observed that the task-space error converges to a value less than 3mm of the desired trajectory position after about 0.3 seconds.

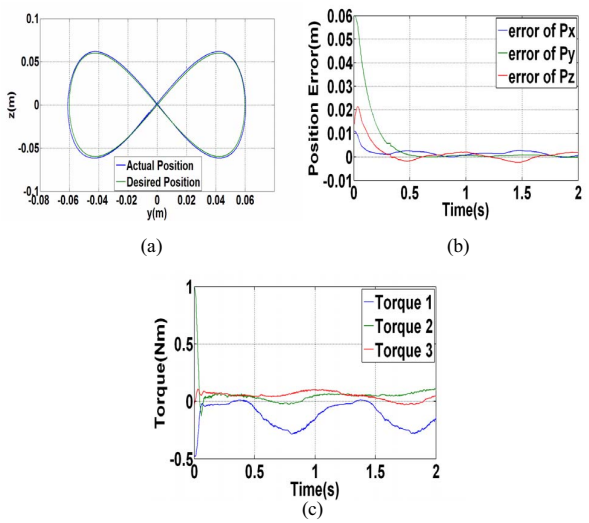

Figure 5. (a) Position error plot, and (b) parametric plot of actual and desired task-space positions, and (c) joint torques

VI. CONCLUSION

In this paper, a computationally simple and compact form of the inverse dynamic model of the Omega-3 parallel manipulator was developed using the principle of virtual work. In order to create the model a simplifying hypothesis proposed in [15] was applied. A simplified solution for the inverse kinematics was also provided by applying the concept of the loop closure equation to the problem. Using the compact form of the inverse dynamic model, we created a trajectory-tracking controller, which provided good tracking results with task-space position errors of less than 3mm. Our further work will focus on creating a telerobotic interface between the Omega-3 robot and a user controlled robotic manipulator.

REFERENCES

[1] Y. Li and Q. Xu, "Dynamic analysis of a modified DELTA parallel robot for cardiopulmonary resuscitation," Intelligent Robots and Systems, 2005. (IROS 2005). 2005 IEEE/RSJ International Conference on , Edmonton, Alberta, Canada, 2-6 Aug. 2005, pp. 3371-3376.

[2] C.W. French, E.A. Schultz, "Multi-axial subassemblage testing (Mast) system: description and capabilities", 13th World Conference on Earthquake Engineering, Vancouver, Canada, 1-6 Aug. 2004, Paper No. 2146.

[3] G. Brandt, A. Zimolong, L. Carrat, P. Merloz, H. W. Staudte, S. Lavallee, K. Radermacher, and G. Rau, "CRIGOS: a compact robot for image guided orthopedic surgery," Information Technology in Biomedicine, IEEE Transactions on, vol. 3, no. 4, pp. 252–260, Dec. 1999.

[4] L. W. Tsai, Robot Analysis: The Mechanics of Serial and Parallel Manipulators, John Wiley & Sons, New York. 1999.

[5] J. P. Merlet, Parallel Robots. London: Kluwer Academic Publishers, 2000.

[6] Y. Li and G.M. Bone, "Are parallel manipulators more energy efficient?," Computational Intelligence in Robotics and Automation, 2001. Proceedings 2001 IEEE International Symposium on, pp. 41-46, 2001.

[7] W. Q. D. Do and D. C. H. Yang, "Inverse dynamic analysis and simulation of a platform type of robot," Journal of Robotic Systems, , vol. 5, no. 3, pp. 209–227, 1988.

[8] P. Guglielmetti and R. Longchamp, "A closed form inverse dynamics model of the Delta parallel robot," Proceedings of Symposium on Robot Control, pp. 51–56, 1994.

[9] K. Y. Tsai and D. Kohli, "Modified Newton-Euler computational scheme for dynamic analysis and simulation of parallel manipulators with applications to configuration based on R-L actuators," Proceedings ASME Design Engineering Technical Conferences, vol. 24, pp. 111–117, 1990.

[10] M. Ahmadi, M. Dehghani, M. Eghtesad, and A.R. Khayatian, "Inverse dynamics of HEXA parallel robot using Lagrangian dynamics formulation," Intelligent Engineering Systems, 2008. INES 2008. International Conference on, pp.145-149, 25-29 Feb. 2008.

[11] G. Lebret, K. Liu, and F.L. Lewis, "Dynamic analysis and control of a stewart platform manipulator," Journal of Robotic Systems, vol. 10, no. 5, pp. 629–655, 1993.

[12] K. Miller, and R. Clavel, "The Lagrange-based model of Delta-4 robot dynamics," Robotersysteme, Springer-Verlag, 8, pp. 49-54, 1992.

[13] H. Pang and M. Shahingpoor, "Inverse dynamics of a parallel manipulator," Journal of Robotics Systems, vol. 11, no. 8, pp. 693-702, 1994.

[14] Y. Li and Q. Xu, "Kinematics and inverse dynamics analysis for a general 3-PRS spatial parallel mechanism," Robotica, vol. 23, no. 2, pp. 219-229, 2005.

[15] A. Codourey, "Dynamic modeling and mass matrix evaluation of the DELTA parallel robot for axes decoupling control," Intelligent Robots and Systems '96, IROS 96, Proceedings of the 1996 IEEE/RSJ International Conference on , vol.3, pp. 1211-1218, 4-8 Nov 1996.

[16] L. W. Tsai, "Solving the inverse dynamics of a Stewart-Gough manipulator by the principle of virtual work," ASME Journal of Mechanical Design, vol. 122, no. 1, pp. 3-9, 2000.

[17] K.E. Zanganeh, R. Sinatra, and J. Angeles, "Kinematics and dynamics of a six-degree-of-freedom parallel manipulator with revolute legs," Robotica, vol. 15, pp. 385–394, 1997.

[18] J. Wang and C.M. Gosselin, "Dynamic analysis of spatial four-degree-of-freedom parallel manipulators," ASME Design Engineering Technical, Sacramento, CA, Paper No. DETC97/DAC3759, 1997.

[19] R. Clavel, "DELTA, a fast robot with parallel geometry," In 18th Int. Symposium on Industrial Robots and Systems (IROS), Lausanne, pp. 91-100, 26-28 April, 1988.

[20] J. P. Lallemand, A. Goudali and S. Zeghloul, "The 6-DOF 2-Delta parallel robot," Robotica, vol. 15, no. 4, pp. 407-416, 1997.

[21] St. Staicu, D.C. Carp-Ciocardia, "Dynamic analysis of Clavel's Delta parallel robot," Robotics and Automation, 2003. Proceedings. ICRA '03. IEEE International Conference on , vol. 3, pp. 4116-4121, 14-19 Sept. 2003.

[22] H. Baruh, Analytical Dynamics, WCB McGraw-Hill, 1999.